Metformin coordinates osteoblast/osteoclast differentiation associated with ischemic osteonecrosis

See-Hyoung Park[1,*], Mi-Ae Kang[2,*], Young Jae Moon[3,*], Kyu Yun Jang[4], Jung Ryul Kim[3]

[1]Department of Bio and Chemical Engineering, Hongik University, Sejong, Korea
[2]Department of Biological Science, Gachon University, Seongnam, Korea
[3]Department of Orthopaedic Surgery, Chonbuk National University Medical School, Research Institute of Clinical Medicine of Chonbuk National University-Biomedical Research Institute of Chonbuk National University Hospital and Research Institute for Endocrine Sciences, Jeonju, Korea
[4]Department of Pathology, Chonbuk National University Medical School, Research Institute of Clinical Medicine of Chonbuk National University-Biomedical Research Institute of Chonbuk National University Hospital and Research Institute for Endocrine Sciences, Jeonju, Korea
*Equal contribution

Correspondence to: Jung Ryul Kim, Kyu Yun Jang; **email:** jrkeem@jbnu.ac.kr, kyjang@chonbuk.ac.kr
Keywords: metformin, angiopoietin 1, ischemic osteonecrosis, osteoblastic differentiation
Received: October 27, 2019   **Accepted:** January 12, 2020   **Published:** February 11, 2020

ABSTRACT

In this study, we aimed to identify a candidate drug that can activate endogenous Angiopoietin 1 (Ang1) expression via drug repositioning as a pharmacological treatment for avascular osteonecrosis. After incubation with 821 drugs from the Food and Drug Administration (FDA)-approved drug library, Ang1 expression in U2OS cell culture media was examined by ELISA. Metformin, the first-line medication for treatment of type 2 diabetes, was selected as a candidate for in vitro and in vivo experimental evaluation. Ang1 was induced, and alkaline phosphatase activity was increased by metformin treatment in U2OS and MG63 cells. Wound healing and migration assay showed increased osteoblastic cell mobility by metformin treatment in U2OS and MG63 cells. Metformin upregulated expression of protein markers for osteoblastic differentiation in U2OS and MG63 cells but inhibited osteoclastic differentiation in Raw264.7 cells. Metformin (25 mg/kg) protected against ischemic necrosis in the epiphysis of the rat femoral head by maintaining osteoblast/osteocyte function and vascular density but inhibiting osteoclast activity in the necrotic femoral head. These findings provide novel insight into the specific biomarkers that are targeted and regulated by metformin in osteoblast differentiation and contribute to understanding the effects of these FDA-approved small-molecule drugs as novel therapeutics for ischemic osteonecrosis.

INTRODUCTION

Ischemic necrosis of the femoral head (INFH) can lead to permanent femoral head deformity, severely compromised hip joint longevity, and premature end-stage osteoarthritis as early as the third decade of life. Use of biological agents to preserve the femoral head and avoid joint replacement surgery is currently under investigation. The therapeutic concepts of angiogenesis and secondary osteogenesis have gained considerable attention in terms of preventing development of femoral head deformities after ischemic osteonecrosis [1].

Thus far, several kinds of growth factors have been reported to regulate angiogenesis [2]. Among them, Angiopoietin 1 (Ang1) is a well-known angiogenic factor that plays a pivotal role in stimulating and developing new vasculature for bone formation [3, 4].

Previously, we reported that a recombinant COMP-Ang1 protein, a chimeric form of Ang1, facilitates necrotic femoral head repair via enhancement of angiogenesis [5].

It is both expensive and time-consuming to develop new drugs [6]. Recently, a novel concept called "Drug Repositioning or Repurposing" has been introduced to find and develop new drugs [7]. This approach applies clinically used drugs to other specific diseases by elucidating new activity and target molecules [8]. This has many advantages, such as no need to test toxicity or evaluate pharmacokinetics [9]. These advantages can considerably reduce the cost and time to develop new drugs, leading to improved success rates [10]. In this study, we adapted the drug repositioning concept to identify candidate drugs to promote differentiation of osteoblast-like cells by inducing Ang1 expression. We selected metformin as such a candidate after screening an FDA-approved drug library with ELISA.

Metformin is currently used as a primary drug for treatment of Type 2 diabetes [11], especially for overweight or obese patients with normal renal function [12]. Metformin improves blood sugar level [13] by activating AMP-activated protein kinase (AMPK) [14] in the liver, thereby inhibiting biosynthesis of fatty acids [15], promoting glucose uptake into cells [16] and inhibiting metabolic syndrome [17]. In this study, we demonstrated that metformin induced osteoblast differentiation and suppressed osteoclast differentiation in an in vitro cell model. Furthermore, metformin prevented femoral head deformity through induction of angiogenesis in an in vivo INFH rat model. Our results provide an effective therapeutic strategy for treatment of INFH via drug repositioning.

RESULTS

Metformin increases Ang1 expression and cell mobility in U2OS and MG63 cells

Ang1 expression was examined by ELISA in U2OS cells [18] after treatment with a library of 821 FDA-approved drugs (Figure 1A and Table 1), and metformin was selected as one of the strongest candidates. As shown in Figure 1B, metformin increased Ang1 expression in U2OS and MG63 cells. The expression level of Ang1 protein in both cell types was upregulated significantly in a dose-dependent manner in metformin-treated groups. To confirm that Ang1 expression was induced by metformin treatment in U2OS and MG63 cells, total proteins were condensed and analyzed by Western blotting of cell culture media from U2OS and MG63 cells treated with or without metformin. Compared to the DMSO vehicle control, 5 μM of metformin notably increased Ang1 expression in U2OS and MG63 cells. While metformin increased Ang1 expression, angiopoietin2 expression did not differ, implying that metformin is specific for Ang1 expression (Figure 1C). Since proangiogenic Ang1 expression was enhanced by metformin in U2OS and MG63 cells, we tested whether cell mobility (an angiogenic result) of U2OS and MG63 was affected by metformin. As shown in Figure 1D, the membrane-traversed U2OS and MG63 cells were increased by metformin dose-dependently. In addition, the wound healing assay results showed a significant promotion in wound closure following treatment with metformin in U2OS and MG63 cells (Figure 1E).

Metformin accelerates osteoblast mineralization and upregulates osteoblast differentiation in U2OS and MG63 cells

As shown in Figure 2A, ALP activity in metformin-treated (2.5, 5, and 10 μM) U2OS and MG63 cells was significantly higher than in DMSO-treated cells. Osteoblast mineralization refers to deposition of copious amounts of extracellular calcium, which is thought to be essential for bone formation [19]. Metformin treatment for 20 days increased alizarin red S-stained U2OS and MG63 cells in a dose-dependent manner (Figure 2B). Quantification of alizarin red S staining indicated a significant increase in staining after 5 uM metformin treatment compared with DMSO treatment (Figure 2C). These results suggest that metformin enhances osteoblast differen-tiation and mineralization *in vitro*. As shown in Figure 2D, compared with DMSO vehicle control, 5 μM of metformin notably increased COL1A1, OC, BSP, Dlx5, Runx2, and OSX expression in U2OS and MG63 cells. Moreover, ALP expression level was were dramatically, consistent with the changes in ALP activity.

Metformin induces phosphorylation of p38

p38 MAPK is reported to interact physically with and transcriptionally activate Runx2 [20] and OSX [21] during osteoblastic differentiation. Thus, we examined whether metformin can induce phosphorylation (activation) of p38 MAPK in U2OS and MG63 cells. As shown in Figure 3A, metformin increased the phosphorylated form of p38 MAPK (p-p38 MAPK) in a dose-dependent manner. Then, we investigated protein interactions between p38 MAPK and Runx2 or OSX after treating U2OS and MG63 cells with metformin. As shown in Figure 3B, p-p38 MAPK expression was much higher and the amount of p38 MAPK protein interacting with Runx2 or OSX was increased by metformin in U2OS and MG63 cells. These results
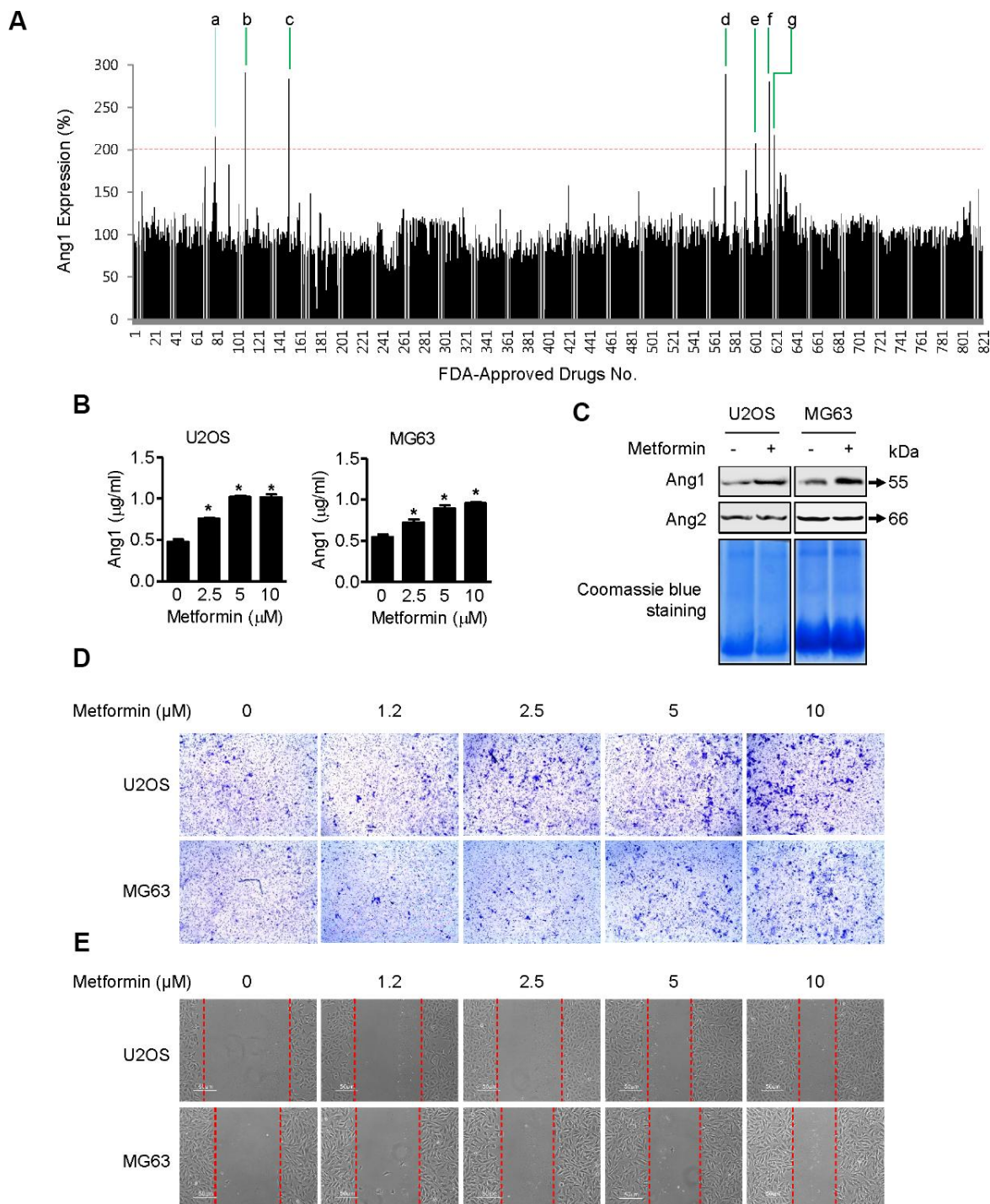
Figure 1. Induction of Ang1 expression and activation of cell mobility by metformin. (**A**) Screening result of FDA-approved drugs for Ang1 expression by ELISA. U2OS cells were seeded on 96-well plates. After treating cells with drugs for 1 h, each cell culture medium was transferred to a 96-well plate from the ELISA assay kit. Compounds that induced Ang1 expression over two-fold compared with DMSO vehicle control were selected and are listed in Table 1. (**B**) U2OS and MG63 cells were treated with 2.5, 5, and 10 μM of metformin or an equal volume of DMSO (0.1%) for 1 h. Cell culture medium was collected for Ang1 ELISA. Significant differences between metformin and DMSO control groups are indicated (*$P < 0.05$, a paired t-test). Experiments were performed in triplicate, and error bars represent standard deviation. (**C**) Cells were treated with 5 μM of metformin or an equal volume of DMSO (0.1%) for 1 h. Cell culture medium from the treated cells was condensed with a Microcon for Western blotting. Coomassie blue staining of SDS-PAGE gels was used for a loading control. Ang1: Angiopoetin1, Ang2: Angipoietin2. (**D**, **E**) (**D**) U2OS and MG63 cells were treated with 2.5, 5, and 10 μM of metformin or an equal volume of DMSO (0.1%) for 6 h. The membrane-traversed cells were fixed and stained with crystal violet solution. (**E**) Cell migration was observed and captured by microscopy at the indicated time point.

Table 1. Selected drug candidates from the screening for Ang1 expression.

No.	Drugs	Position	Application
a	Tolcapone	1-H10	Antiparkinson
b	Metformin·HCl	2-C09	Antidiabetic
c	Sodium Phenylbutyrate	2-G11	Antineoplastic
d	Flucytosine	8-B03	Antimycotic
e	Hydroxyzine Dihydrochloride	8-E02	Antihistamine
f	Lacosamide	8-F05	Anticonvulsant
g	Leucovorin Calcium Pentahydrate	8-F10	Antitoxicity

suggest that metformin upregulates transcriptional activity of both Runx2 and OSX proteins via activation of p38 MAPK, leading to high expression of other proteins such as COL1A1, OC, BSP, and Dlx5 for osteoblastic differentiation.

Metformin inhibits osteoclast differentiation in RAW264.7 cells

As shown in Figure 4A, IL-6 expression was decreased by metformin in RAW264.7 cells compared
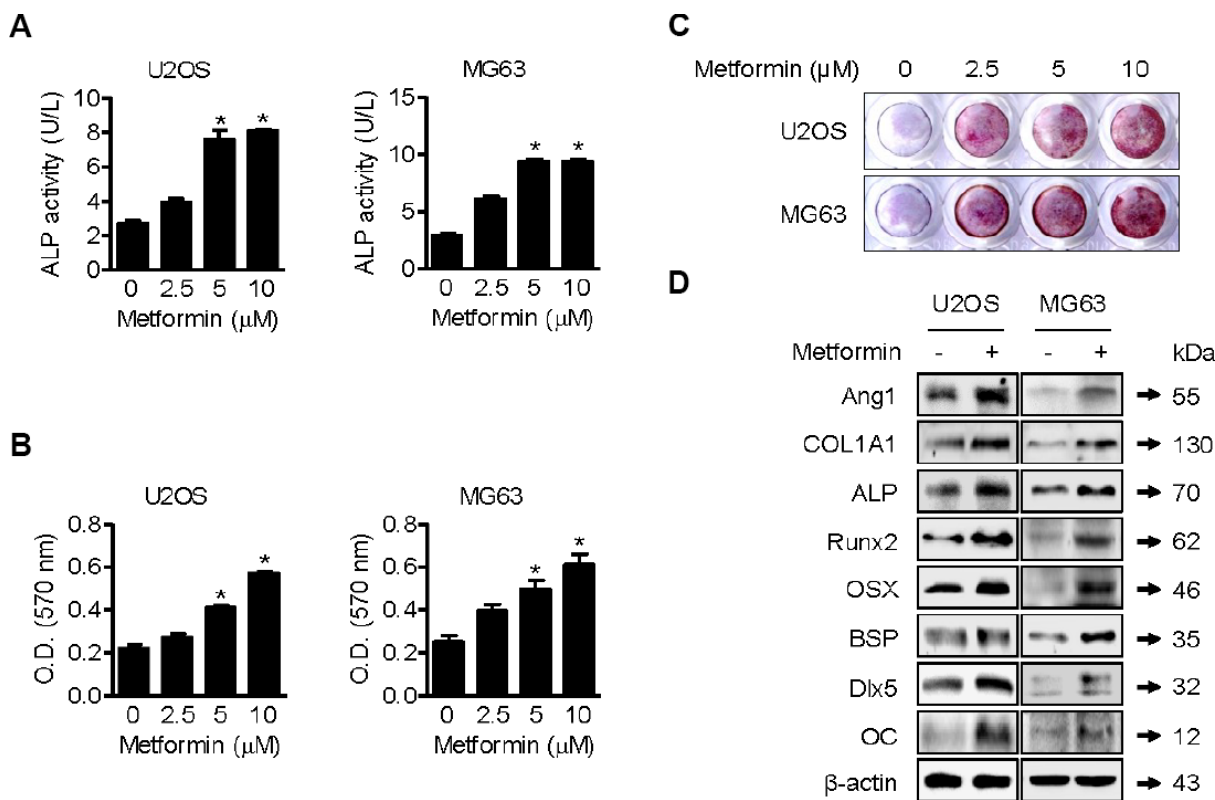
Figure 2. Promotion of osteoblast mineralization by metformin. (**A**–**C**) U2OS and MG63 cells were treated with 2.5, 5, and 10 μM of metformin or an equal volume of DMSO (0.1%) for 1 h (**A**) and (**B** and **C**) 20 days. ALP activity in cells was analyzed. Significant differences between metformin and DMSO control groups are indicated (*$P < 0.05$, a paired t-test). Experiments were performed in triplicate, and the error bars represent standard deviation. (**B**) Cell culture medium containing the proper amount of metformin was changed every other day. The cells were then fixed and stained by Alizarin Red S. (**C**) Alizarin red S-stained cells were extracted, and the optical density was measured with a microplate reader. Significant differences between metformin and DMSO control groups are indicated (*$P < 0.05$, a paired t-test). Experiments were performed in triplicate, and the error bars represent standard deviation. (**D**) For Western blotting analysis of protein markers of osteoblast differentiation, cells were treated with 5 μM of metformin or an equal volume of DMSO (0.1%) for 1 h. Cells were harvested, and the lysed proteins were resolved on SDS-PAGE and immunoblotted with specific antibodies.

with DMSO control. We next investigated control of IL-6 expression by metformin in RAW264.7 cells in more detail. For this purpose, we performed Western blots of IL-6, p-Iκbα, Iκbα, IKKβ, and NFκB p65. NFκB p65 is a well-known transcription factor that regulates IL-6 expression in osteoclast cells. As shown in Figure 4B, IL-6, p-Iκbα, IKKβ, and NFκB p65 were downregulated by metformin, whereas Iκbα was unchanged. These results imply that NFκB p65 transcriptional activity was reduced through inhibition of IKKβ, leading to the decrease in IL-6 expression. In addition, as shown Figure 4B, expression levels of c-Src, TRAP, and Cathepsin K, well-known protein markers for osteoclast differentiation, were reduced by metformin in RAW264.7 cells. This is consistent with the above IL-6 expression results in terms of preventing differentiation of RAW264.7 cells into osteoclast cells. For measuring TRAP-positive multinucleated RAW264.7 cells, cells were incubated with recombinant RANKL and metformin for 2 or 7 days. As shown in Figure 4C and 4D, metformin decreased TRAP-positive multinucleated cells in a dose-dependent manner that was confirmed by the TRAP activity assay (Figure 4E).

Metformin protects against ischemic necrosis in the epiphysis of the femoral head

Although there was no significant difference in body weight or general condition between the metformin-injected and control groups, partial absorption of the femoral head epiphysis was observed in the surgery-induced ischemic necrosis of femoral head (INFH) control group (Figure 5A). However, the INFH metformin-injected group showed intact epiphysis of the femoral head, similar to the sham group (Figure 5A). µCT analysis showed decreased bone volume per tissue volume and trabecular number and increased total porosity in the INFH control group compared with the sham group (Figure 5B). On the other hand, bone volume per tissue volume and trabecular number were significantly increased in the INFH with metformin group compared with the INFH control. Moreover, trabecular separation and total porosity were significantly decreased in the INFH with metformin group (Figure 5B). H & E staining and Safranin-O staining showed destruction of the cartilage of the femoral head and accumulation of inflammatory cells in the INFH control. However, the femoral head was intact
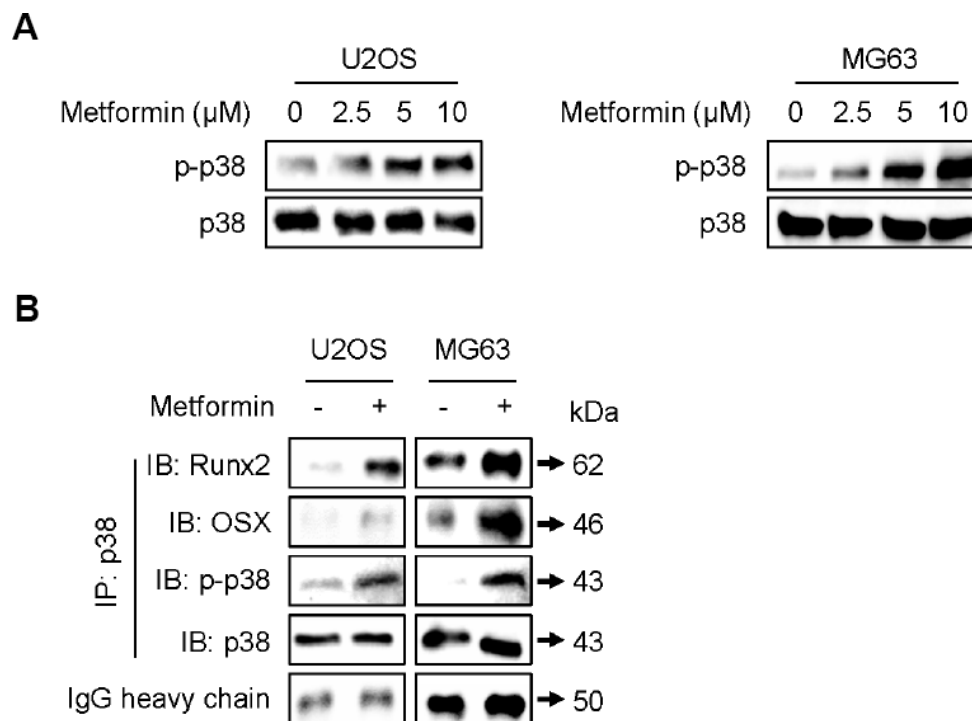
Figure 3. Increase in phosphorylation of p38 by metformin. (**A**) Cells were treated with 2.5, 5, and 10 µM of metformin or an equal volume of DMSO (0.1%) for 1 h. Cells were harvested, and the lysed proteins were resolved on SDS-PAGE and immunoblotted with specific antibodies against p-p38 MAPK and p38 MAPK. (**B**) For immunoprecipitation analysis, cells were treated with 5 µM of metformin or an equal volume of DMSO (0.1%) for 1 h. Cells were harvested, and the lysed proteins were immunoprecipitated with antibody against p38 MAPK. The immunoprecipitated proteins were resolved on SDS-PAGE and immunoblotted with specific antibodies against Runx2, OSX, p-p38 MAPK, and p38 MAPK. IgG heavy chain blotting was used as a loading control.

in INFH with metformin group (Figure 5C). These results suggest that injection of metformin has protective effects against surgery-induced INFH in rats.

Metformin maintains osteoblast/osteocyte function and vascular density but inhibits osteoclast activity in epiphyseal bone

To determine the basis of the protective effect of metformin in INFH, we performed immuno-histochemical staining in paraffin sections of femoral heads. The expression of ALPL, which is a pre-osteoblast marker, and DMP1, which is a mature osteoblast marker, was reduced in INFH control (Figure 6A). However, the INFH with metformin group showed similar expression of ALPL and DMP1 to the sham group. To evaluate the effects of metformin on femoral head vascularity, femoral heads were immunostained for vWF, a marker of endothelial cells of blood vessels.

Immunostaining for vWF antigen revealed more blood vessels in INFH with metformin compared with the INFH control (Figure 6A). Similarly, vascular density was significantly increased in the INFH with metformin group compared with INFH controls (Figure 6B). These results suggest that metformin has a protective role in INFH caused by maintenance of osteoblast function and vascular density. Because of bone destruction in AVN due to osteoclast activity, we evaluated osteoclast activity using TRAP staining. The TRAP-positive cells were increased in INFH controls but decreased in the INFH with metformin group (Figure 6C).

DISCUSSION

Although there are numerous studies on the anti-angiogenic activity of metformin in cancer models [22–24], we focused on the pro-angiogenic effect of metformin by induction of Ang1 expression in osteo-
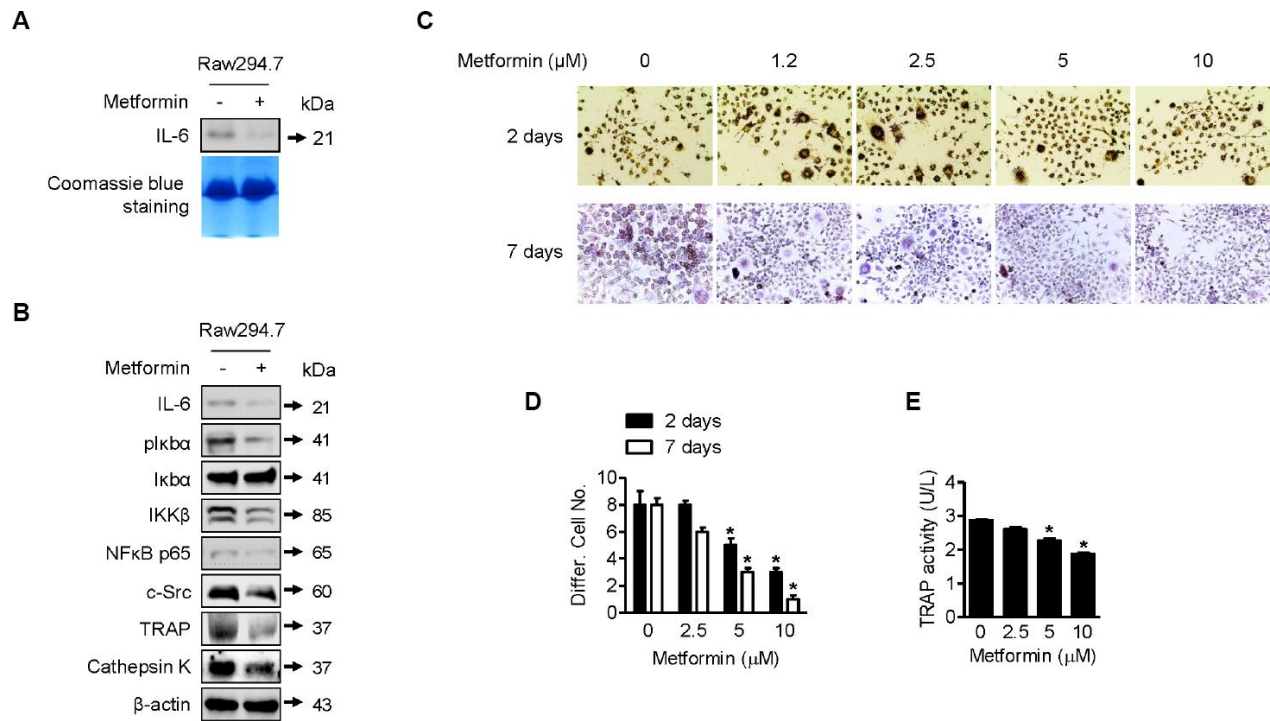
Figure 4. Downregulation of osteoclast differentiation by metformin. (**A**) For Western blotting analysis of IL-6 expression by metformin in RAW264.7 cells, cells were treated with 5 μM of metformin or an equal volume of DMSO (0.1%) for 1 h. Cell culture medium from the treated cells was condensed with a Microcon for Western blotting. Coomassie blue staining of SDS-PAGE gels were used for a loading control. (**B**) For Western blotting analysis, cells were treated with 5 μM of metformin or an equal volume of DMSO (0.1%) for 1 h. Cells were harvested, and the lysed proteins were resolved on SDS-PAGE and immunoblotted with specific antibodies against IL-6, pIκbα, Iκbα, IKKβ, NFκB p65, c-Src, TRAP, and Cathepsin K. β-actin blotting was used as a loading control. (**C**) Cells were treated with 2.5, 5, and 10 μM of metformin or an equal volume of DMSO (0.1%) with or without RANKL (0.1 μg/ml) for 2 or 7 days. During incubation, cell culture medium containing the proper amount of metformin was changed every other day. Cells were fixed and stained by the TRAP staining kit according to the manufacturer's manual. For quantitative comparison, multinucleated cells were counted (**D**). (**E**) RAW264.7 cells were treated with 2.5, 5, and 10 μM of metformin or an equal volume of DMSO (0.1%) for 1 h. TRAP activity in cells was analyzed according to the manufacturer's protocol. Significant differences between metformin and DMSO control groups are indicated (*$P < 0.05$, a paired t-test). Experiments were performed in triplicate, and the error bars represent standard deviation.

blastic cells. In the same vein as our finding on activation of angiogenesis to overcome ischemic conditions in the femoral head, many publications describe a similar approach using metformin to treat ischemic conditions in the brain [25–27]. Ischemic stroke is a major cause of death and disability. For potential therapeutic strategies, researchers have discovered that chronic administration of metformin prevents ischemic stroke in a mouse model [28]. Its mechanism of action has not been elucidated in detail, but chronic treatment with metformin paradoxically inhibits AMPK in ischemic stroke mouse models. Thus, there seems to be unidentified pleiotropic mechanisms of metformin involved in regulation of other diseases. Recently, Abdelsaid et al. showed the potential of metformin to restore angiogenesis in the brain of a rat model with diabetes [29]. They induced ischemic injury in diabetic rats and treated them with metformin. They demonstrated that the excess peroxynitrite formed by ischemia injury in diabetic rats causes brain cell apoptosis in the period after stroke, and metformin prevents this nitrative stress and restores angiogenic function in brain tissue, as evaluated by wound healing and tubule formation assays from primary culture endothelial cells from rats. Thus, the pharmacological functions and mechanisms of metformin via activation
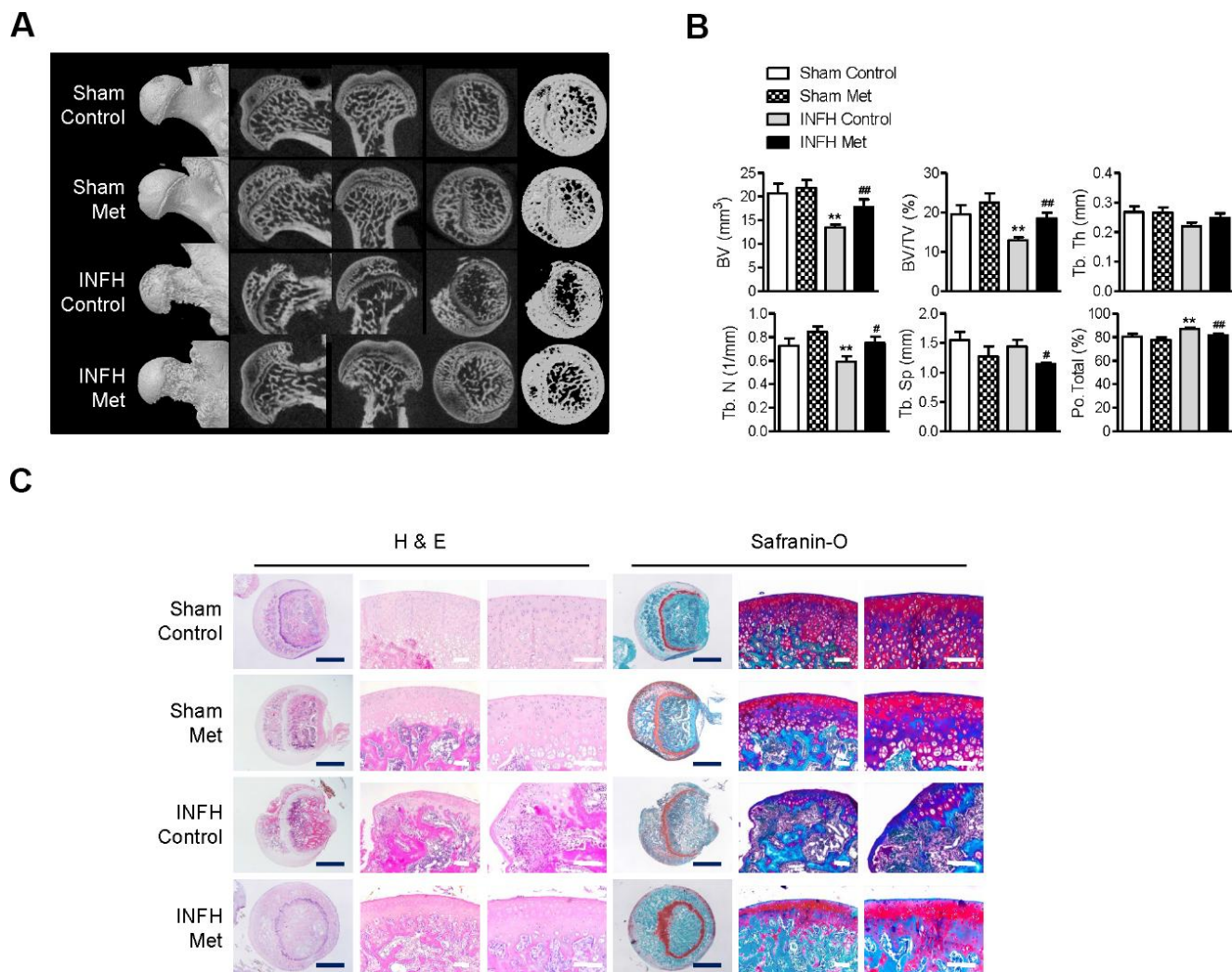

Figure 5. Protective effect of metformin in the INFH rat model. (A) Representative images of μCT in sham-operated rats with saline injection (Sham Control), sham-operated rats with metformin injection (Sham Met), INFH-operated rats with saline injection (INFH Control), and INFH-operated rats with metformin injection (INFH Met). Images are arranged in order of 3D μCT reconstructions of femoral head area and the coronal, sagittal, and middle areas of femoral heads. (B) Morphometric indices in femoral heads of the four groups. Values are presented as the mean ± STD (n = 5). **$p < 0.001$ versus Sham Control, #$p < 0.01$ and ##$p < 0.001$ versus INFH Control. (C) Representative images of H & E and Safranin-O staining in the four groups. Black bars = 500 μm, white bars = 50 μm. Abbreviations: BV, bone volume; Tb. N, trabecular number; Tb.Sp, trabecular separation; Tb.Th, trabecular thickness; TV, tissue volume; Po, porosity.

of angiogenesis may lead to neuroprotection in cerebral ischemia. As shown in Figure 1D and 1F, we observed dose- and time-dependently increased cell mobility when U2OS and MG63 cells were incubated with metformin. However, it is still not clear whether Ang1 induced by metformin or metformin itself directly affects cell mobility.

Accumulating evidence indicates that patients with diabetes are exposed to higher risk of bone fractures. Although several observational studies have been performed to investigate this relationship, the main risk factors for fracture from diabetes are still not identified [30–32]. A recent meta-analysis study to address the therapeutic effects of seven clinically used anti-diabetic drugs on fractures showed that thiazolidinediones significantly increase fracture risk in older women, but metformin seemed to have no effect on the incidence of bone fracture in patients with diabetes [33].

Metformin, a first-line medication for type 2 diabetes, has been shown to have potential for osteogenic differentiation. A recent study demonstrated that metformin promotes osteogenic differentiation and mineralization of mesenchymal stem cells [34]. That study showed that metformin significantly enhanced ALP activity, mineralized nodule formation, and expression of Runx2 and OSX, consistent with our data (Figure 2A–2C) in an osteoblast cell line. Interestingly, they elucidated the details of the molecular mechanism by examining the effect of metformin on the signaling pathway of LKB1/AMPK, which contains well-established target proteins activated by metformin. Thus, to expand our study, we tested whether metformin affects activation of the LKB1/AMPK signaling pathway in U2OS and MG63 cells. Xinyu et al. reported that, under high-glucose cell culture media, the proliferation rate of MG63 osteoblast cells was lower than under normal-glucose cell culture media, and metformin treatment rescued this suppression of proliferation of MG63 cells [35]. By Western blotting and real-time PCR analysis, they also showed that metformin increases expression of COL1A1, OC, and osteoprotegerin (OPG) with enhanced APL enzyme activity in MG63 cells, also consistent with our current study (Figure 2D).
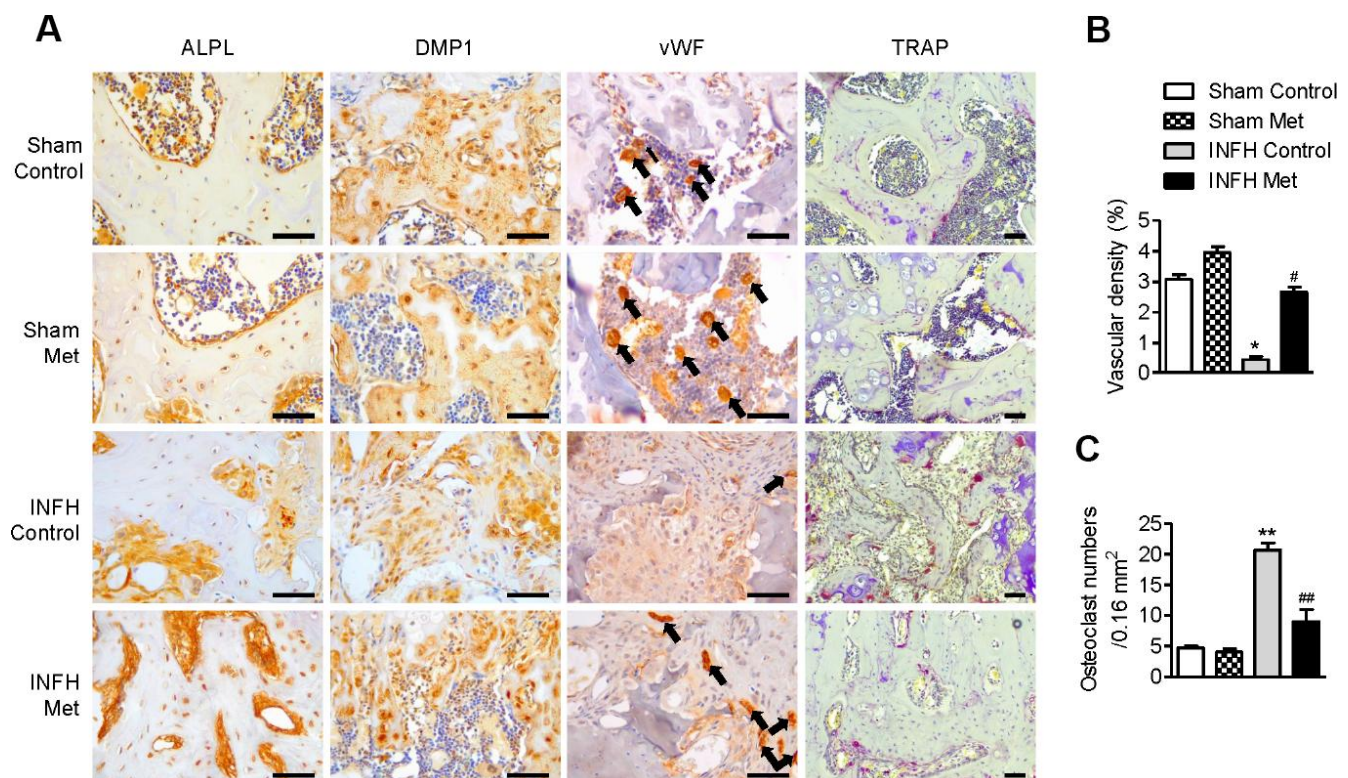
Figure 6. Working mechanism of metformin in the INFH rat model. (A) Immunohistochemical staining of ALPL, DMP1, vWF, and TRAP in the femoral head epiphysis. Black arrows indicate positive expression of vWF, a marker of endothelial cells of blood vessels. (B) Percentage of vascular density in the four groups. Vascular density (%) was calculated as vascular area stained by antibody for vWF-related antigen/total area of each image. Values are presented as the mean ± STD. (n = 4). *$p < 0.01$ versus Sham Control, #$p < 0.01$ versus INFH Control. (C) Number of TRAP-positive cells per unit area. Values are presented as the mean ± STD (n = 4). **$p < 0.001$ versus Sham Control, ##$p < 0.001$ versus INFH Control. Black bars = 50 μm.

p38 MAPK has been reported to play a key role in osteoblast differentiation. For example, p38 MAPK is phosphorylated (activated) during osteoblast differentiation in human mesenchymal stem cells [36]. SB203580, a pharmacological inhibitor of p38 MAPK, impairs osteoblast differentiation of MC3T3 cells and downregulates expression of ALP, OC, and COL1A1 [37, 38]. As *in vivo* evidence for activation of p38 MAPK in osteoblast differentiation, several reports have shown that p38 MAPK knock-out transgenic mice have impaired osteoblast differentiation, bone composition, and maintenance [39, 40]. As described in the results section of our study (Figure 3A and 3B), p38 MAPK is phosphorylated by metformin treatment to show stronger binding to Runx2 [20] and OSX [21], which seems to increase their transcriptional activity during osteoblastic differentiation. Previously, Ge et al. demonstrated that p38 MAPK phosphorylates Ser319 of Runx2 using a specific phospho-Runx2 antibody and activates the transcriptional activity of Runx2 according to luciferase assay analysis, leading to osteoblast differentiation [41]. In other reports, p38 MAPK phosphorylated Ser33 and Ser77 of OSX and activated transcriptional activity of OSX via recruitment of p300 and BRG-1 [42, 43]. As shown in Figure 3B, protein interactions between p38 MAPK and Runx2 or OSX were increased with phosphorylation of p38 MAPK by metformin in U2OS and MG63 cells, possibly representing the enhanced transcriptional ability of Runx2 and OSX for regulating other genes related to osteoblast differentiation such as COL1A1, OC, BSP, and Dlx5. At present, we are trying to verify whether Runx2 and OSX bind to and cooperate with each other to increase their protein stability and to locate the cell nucleus for transcriptional activity by metformin. Artigas et al. reported that this interaction requires action of p38 MAPK, and mutant phosphorylation sites of Runx2 and OSX prevented their interaction [44]. However, it is still not clear whether metformin-induced Ang1 or metformin itself directly affects phosphorylation of p38 MAPK with transcriptional activation of Runx2 and OSX. This issue may be resolved using cell lines and mouse models with Ang1 knock-down or knock-out. Considering the number of key actions of p38 MAPK in bone development, we focused on p38 MAPK activation by metformin as a central working mechanism of osteogenesis.

Bone remodeling is the result of a balance between osteoblast and osteoclast differentiation. Thus, a strategy for developing optimal therapies for ischemic osteonecrosis might target either activation of osteoblasts or inhibition of osteoclasts. Osteoclast differentiation is regulated by inflammatory factors and hormones [45]. Among various inflammatory factors, IL-6 has been actively studied and is known to be closely related to osteoclast differentiation [46, 47]. Furthermore, IL-6 may stimulate osteoblast cells to express RANKL to enhance osteoclast differentiation [47]. Therefore, we aimed to investigate IL-6 expression in RAW264.7 osteoclast cells by metformin treatment. As shown in Figure 4A and 4B, IL-6 was less expressed and secreted when RAW264.7 osteoclast cells were incubated with metformin. This result suggests that metformin inhibits osteoclast differentiation via downregulation of IL-6, which was confirmed by other protein markers for osteoclast differentiation and a TRAP assay (Figure 4). Although we showed the NFκB/IKKβ signaling pathway to be involved in regulation of IL-6 expression in RAW264.7 cells by metformin, we need to assess other signaling pathways controlled by IL-6 in osteoclast cells. According to a recent study, IL-6 can activate Janus activated kinase (JAK), leading to phosphorylation of signal transducer and activator of transcription 3 (STAT3) transcription factor, which is responsible for RANKL expression [48]. Thus, we are investigating regulation of the IL-6/JAK/STAT3/RANKL pathway in osteoclast cells with metformin. Hye-Jin et al. demonstrated the anti-arthritis activity of metformin via downregulation of IL-17-producing T cells (Th17) and upregulation of regulatory T cells (Treg) in a collagen-induced arthritis (CIA) mouse model [49]. According to them, metformin administration suppressed osteoclastogenic activity in CIA and expression of genes related to osteoclast differentiation such as RANKL, TRAP, MMP-9, integrin 3, calcitonin receptor, and Cathepsin K, which is consistent with our Western blot analysis (Figure 4B), and osteoclastogenic activity in CIA. These results indicate that metformin is a potential therapeutic option for rheumatoid arthritis and ischemic osteonecrosis.

In our in vivo findings, administration of metformin after ischemic necrosis surgery maintained osteoblast/ osteocyte function and vascular density and suppressed osteoclast activity compared to controls. These effects of metformin had a protective role in ischemic osteonecrosis. Our findings supported those of various other in vivo models. First, metformin increased bone healing mediated by Runx2 and AMPK activation after uniform craniotomy in control and diabetic rats [50]. Furthermore, AMPK knockout mice had smaller cortical and trabecular bone mass compared to WT mice [51]. Second, metformin prevented bone loss in ovariectomized rats through regulation of osteoclastogenesis [52, 53]. Third, metformin induced reduction of alveolar bone loss in ligature-induced periodontitis compared to vehicle-treated rats [54]. These data and our results suggest that metformin has a beneficial effect on bone disease. However, high concentration of metformin (200 mg/kg/day) had no

effect on bone defects induced by periodontitis or fracture healing [54, 55]. Aurigena et al. suggested that low concentration of metformin (50 mg/kg/day) decreased the inflammatory response, oxidative stress, and bone loss in ligature-induced periodontitis in rats [54]. In addition, very low dose of metformin (10 mg/kg/day) prevented bone loss induced by perio-dontitis by increasing osteoblast differentiation [56]. Thus, we used low-dose metformin (25 mg/kg/day) in an INFH rat model.

Overall, we demonstrated that metformin increases Ang1 expression and induces bone formation, differentiation, and mineralization in U2OS and MG63 cell lines *in vitro* and increases vascularity and new bone formation in ischemic femoral heads *in vivo* (Figures 5 and 6). This study reveals a new aspect of metformin by providing novel insight into the specific biomarkers that it regulates during osteoblast/osteoclast differentiation. Since metformin is already widely used for patients with diabetes, this research contributes to the expansion of treatment options for ischemic osteonecrosis.

MATERIALS AND METHODS

Reagents

Metformin, dimethyl sulfoxide (DMSO), glycerol, glycine, sodium chloride, sodium dodecyl sulfate, Trizma base, and Tween20 were purchased from Sigma (St. Louis, MO, USA). The FDA-approved drug library (SCREEN-WELL® FDA-approved drug library V2) was purchased from Enzo Life Sciences (Farmingdale, NY, USA).

Cell culture

U2OS, MG63, and RAW264.7 cell lines (ATCC, Manassas, VA, USA) were cultured in Dulbecco's modified Eagle's medium (DMEM; Invitrogen, Carlsbad, CA, USA) with 10% fetal bovine serum (FBS; Invitrogen) and 1% streptomycin/penicillin (Invitrogen) at 37°C in 5% CO_2.

ELISA analysis

Based on our previous report [18], Ang1 level in cell supernatant was measured with a sandwich ELISA kit (Abcam, Cambridge, MA, USA).

Wound healing assay analysis

U2OS and MG63 cells (1×10^5 per well) were seeded in 6-well plates and cultured with serum-free medium 18 h before assay. Then, an artificial wound was scratched into the confluent cells using a P200 pipette tip.

Microscopy images (Leica DM IL LED; Leica GmbH, Wetzlar, Germany) were collected immediately for a record of 0 h status, cell culture media was replaced with DMEM supplemented with 1% FBS, and cells were treated with vehicle control or metformin. Migration of cells was observed and captured by microscopy at the indicated time point.

Migration assay analysis

U2OS and MG63 cells (1×10^5 per well) were seeded in the upper chamber of the chamber migration apparatus (pore size: 8 μm; Corning Life Sciences, Lowell, MA, USA) and cultured with serum-free medium. Then, cells were treated with the vehicle control or metformin in serum-free medium. After 6 h, cells that had traversed the membrane were fixed and stained with crystal violet solution.

Alkaline phosphatase (ALP) assay analysis

Based on our previous report [18], ALP activity in U2OS and MG63 cells was determined. U2OS and MG63 cells (1×10^5 per well) were seeded in 6-well plates and treated with vehicle control or metformin for 1 h. ALP activity in cells was determined with an ALP activity detection kit (Abcam Inc.). Briefly, the collected cells were washed with PBS, lysed, and centrifuged. The soluble fraction was used for an enzymatic assay. The soluble fraction (80 μL) and 50 μL of 5 mM pNPP substrate were added to 96-well plates and incubated in the dark for 1 h at 25°C. The reaction was stopped by adding 20 μl of stopping solution. The optical density of each sample was measured at 405 nm in a microplate reader (Bio-Rad, Hercules, CA, USA).

Alizarin Red S staining analysis

Based on our previous report [18], U2OS and MG63 cells were stained and analyzed. U2OS and MG63 cells (1×10^4 per well) were seeded into 96-well plates and treated with vehicle control or metformin for 20 days. The medium was changed every other day, and additional cannabidiol was added with each media change. Cells were fixed on day 20 with 4% paraformaldehyde (Sigma) for 15 min at 20°C. Cells were rinsed twice with deionized water (ddH2O) and reacted with 40 mM Alizarin Red S (Sigma) solution in ddH2O (pH 4.2) for 15 min. Cells were washed twice with ddH2O, and images were captured. For quantitative comparison, stained cells were extracted with 10% (w/v) acetyl pyridinium chloride (Sigma) in ddH2O for 30 min, and the optical density of the samples was measured at 570 nm in a microplate reader (Bio-Rad).

Western blotting and immunoprecipitation analysis

U2OS and MG63 cells (1×10^5 per well) were seeded in 6-well plates and treated with vehicle control or metformin. Cells were harvested and lysed with RIPA buffer (Cell Signaling Technology, Danvers, MA, USA). Culture media from the treated cells were condensed with a Microcon YM-10 (Millipore, Bedford, MA, USA) for Ang1 Western blotting analysis. Protein concentrations were determined with a Bradford assay (Bio-Rad). Each protein sample was separated on 10 or 12% SDS-polyacrylamide gel and transferred to a nitrocellulose membrane (Millipore). After blocking for 1 h with a buffer containing 0.05% Tween20 and 3% bovine serum albumin (Sigma), the membrane was probed with specific antibodies and incubated overnight at 4°C. Primary antibodies against p-p38 MAPK, p38 MAPK, ALP, COL1A1, BSP, OC (Cell Signaling Technology), RUNX2, OSX, Dlx5, β-actin, IL-6, p-Iκbα, Iκbα, IKKβ, NFκB p65, c-Src, TRAP, Cathepsin K (Santa Cruz Biotechnology, Santa Cruz, CA, USA), Ang1, and Ang2 (Abcam) were used at a 1:1000 dilution. For immunoprecipitation analysis, cells were washed twice with PBS and lysed with RIPA buffer. The lysates were centrifuged and incubated with an antibody, followed by addition of protein A- or protein G-agarose slurry (Santa Cruz Biotechnology). Protein A/G beads were collected, washed, and resolved by 10 or 12% SDS-PAGE and analyzed by Western blotting.

TRAP staining analysis

RAW264.7 cells (1×10^3 per well) were seeded in 6-well plates. Cells were treated with 100 ng/mL of RANKL (Sigma) and vehicle control or metformin for 2 or 7 days, fixed in 4% paraformaldehyde, and stained for TRAP activity according to the manufacturer's instructions (Abcam). TRAP-positive multinucleated (nuclei>3) cells were scored as osteoclasts using a microscope (Leica DM IL LED; Leica).

Acid phosphatase (TRAP) activity assay analysis

Acid phosphatase activity of RAW264.7 cells (1×10^5 per well) seeded in 6-well plates was determined with an acid phosphatase activity detection kit (Abcam). Briefly, collected cells were washed with PBS, lysed, and centrifuged. The soluble fraction was used for an enzymatic assay.

Animals and surgical procedure

The Institutional Animal Care and Ethics Committee of Chonbuk National University approved all experimental procedures in this study (Ethics number: CBNU 2017-0108). We used male Sprague-Dawley rats (10 weeks of age, 320-350 g). All rats were caged individually at 22°C and 50% humidity in controlled rooms having 12-h light/dark cycles. For anesthesia, we administered Zoletil (150 mg/kg) through intraperitoneal injection. We performed ischemic osteonecrosis of femoral head surgery (n=10) and sham surgery (n=10), as previously described [5]. To confirm the effect of metformin on INFH, metformin was dissolved in physiologic saline. During the week after surgery, we administered metformin (25 mg/kg) once a day by intraperitoneal injection to the experimental group, whereas only saline (the vehicle) was injected in the control group. Rats were euthanized by exsanguination under sodium pentobarbital anesthesia 4 weeks after surgery.

Micro-computed tomography analysis

Four weeks after surgery, we performed micro-computed tomography (μCT) (1076 Skyscan Micro-CT; Skyscan, Kontich, Belgium) and analyzed the findings with CTAn software (Skyscan). All specimens were tested at a constant threshold (~45 %). Femoral bones were analyzed in the center of the femoral neck from the upper margin of the epiphysis of the femoral head.

Tissue preparation, immunohistochemistry, vascular density measurements, and TRAP staining analysis

Femora dissected from rats were fixed in 10% neutral buffered formalin at 4°C overnight. The specimens were then washed with phosphate-buffered saline and decalcified in 15% EDTA for 2 months, dehydrated, embedded in paraffin, and sectioned at a thickness of 5 μm. We performed staining of slides of sections with hematoxylin and eosin (H&E) or Safranin-O (Sigma) for histological analysis. For immunostaining, sections were deparaffinized, and the EXPOSE Rabbit Specific HRP/DAB Detection IHC kit (Abcam) was used according to the manufacturer's instructions. The sections were stained using antibodies against ALPL (1:50; Proteintech, Rosemont, IL, USA), DMP1 (1:300; Takara Bio, Shiga, Japan), and vWF (1:100; Millipore, Temecula, CA, USA). Vascular density was evaluated by measuring vWF-related antigen-stained areas, acquired at the most vascularized area of the femoral head from each rat without knowledge of the experimental group. Four images were produced from each of the four rats per group. Vascular densities were measured using an image analysis system (analySIS, Soft Imaging Systems, Germany) and calculated as (vWF-stained vascular area/total image area in ×200 magnification) × 100 (%). To observe osteoclasts, TRAP staining was performed with a TRAP staining kit (Sigma) according to the manufacturer's instructions.

Statistical analysis

Data are expressed as mean ± standard deviation of three independent experiments. When the variances were equal, differences between groups were analyzed with a paired t-test in SPSS software (version 19.0; SPSS Inc., Chicago, IL, USA). All statistical tests were two-sided, and P values less than 0.05 were considered statistically significant.

Abbreviations

Ang1: angiopoietin1; Ang2: angiopoietin2; INFH: ischemic necrosis of the femoral head; FDA: Food and Drug Administration; AMPK: 5' adenosine monophosphate-activated protein kinase; COL1A1: alpha-1 type I collagen; OC: osteocalcin; BSP: bone sialoprotein; OSX: osterix; TRAP: tartrate-resistant acid phosphatase; ALPL: alkaline phosphatase; DMP1: dentin matrix acidic phosphoprotein 1; μCT: micro-computed tomography; IL-6: interleukin 6; Iκbα: nuclear factor of kappa light polypeptide gene enhancer in B-cells inhibitor, alpha; IKKβ: inhibitor of nuclear factor kappa-B kinase subunit beta; NFκB: nuclear factor kappa-light-chain-enhancer of activated B cells; H&E: hematoxylin and eosin; vWF: von Willebrand factor; BV: bone volume; Tb. N: trabecular number; Tb.Sp: trabecular separation; Tb.Th: trabecular thickness; TV: tissue volume; Po: porosity.

AUTHOR CONTRIBUTIONS

Conception and design of the study, acquisition of data, or analysis and interpretation of data: SHP, MAK, YJM, KYJ, and JRK; Drafting the article or revising it critically for important intellectual content: SHP, MAK, YJM, KYJ, and JRK; Final approval of the version to be submitted: KYJ and JRK.

CONFLICTS OF INTEREST

The authors declare no conflicts of interest.

FUNDING

REFERENCES

1. Zhou L, Yoon SJ, Jang KY, Moon YJ, Wagle S, Lee KB, Park BH, Kim JR. COMP-angiopoietin1 potentiates the effects of bone morphogenic protein-2 on ischemic necrosis of the femoral head in rats. PLoS One. 2014; 9:e110593.
https://doi.org/10.1371/journal.pone.0110593
PMID:25329960

2. Carano RA, Filvaroff EH. Angiogenesis and bone repair. Drug Discov Today. 2003; 8:980–89.
https://doi.org/10.1016/S1359-6446(03)02866-6
PMID:14643161

3. Suri C, Jones PF, Patan S, Bartunkova S, Maisonpierre PC, Davis S, Sato TN, Yancopoulos GD. Requisite role of angiopoietin-1, a ligand for the TIE2 receptor, during embryonic angiogenesis. Cell. 1996; 87:1171–80.
https://doi.org/10.1016/S0092-8674(00)81813-9
PMID:8980224

4. Suri C, McClain J, Thurston G, McDonald DM, Zhou H, Oldmixon EH, Sato TN, Yancopoulos GD. Increased vascularization in mice overexpressing angiopoietin-1. Science. 1998; 282:468–71.
https://doi.org/10.1126/science.282.5388.468
PMID:9774272

5. Park BH, Jang KY, Kim KH, Song KH, Lee SY, Yoon SJ, Kwon KS, Yoo WH, Koh YJ, Yoon KH, Son HH, Koh GY, Kim JR. COMP-Angiopoietin-1 ameliorates surgery-induced ischemic necrosis of the femoral head in rats. Bone. 2009; 44:886–92.
https://doi.org/10.1016/j.bone.2009.01.366
PMID:19442615

6. DiMasi JA, Hansen RW, Grabowski HG. The price of innovation: new estimates of drug development costs. J Health Econ. 2003; 22:151–85.
https://doi.org/10.1016/S0167-6296(02)00126-1
PMID:12606142

7. Ashburn TT, Thor KB. Drug repositioning: identifying and developing new uses for existing drugs. Nat Rev Drug Discov. 2004; 3:673–83.
https://doi.org/10.1038/nrd1468
PMID:15286734

8. Chow WA, Jiang C, Guan M. Anti-HIV drugs for cancer therapeutics: back to the future? Lancet Oncol. 2009; 10:61–71.
https://doi.org/10.1016/S1470-2045(08)70334-6
PMID:19111246

9. Fagan SC. Drug repurposing for drug development in stroke. Pharmacotherapy. 2010; 30:51S–54S.
https://doi.org/10.1592/phco.30.pt2.51S
PMID:20575622

10. Wooller SK, Benstead-Hume G, Chen X, Ali Y, Pearl FM. Bioinformatics in translational drug discovery. Biosci Rep. 2017; 37:BSR20160180.
https://doi.org/10.1042/BSR20160180
PMID:28487472

11. Thrasher J. Pharmacologic Management of Type 2 Diabetes Mellitus: available Therapies. Am J Cardiol. 2017; 120:S4–16.
https://doi.org/10.1016/j.amjcard.2017.05.009
PMID:28606343

12. Gentile S, Piscitelli P, Viazzi F, Russo G, Ceriello A, Giorda C, Guida P, Fioretto P, Pontremoli R, Strollo F, De Cosmo S, Group TA, and AMD-Annals Study Group. Antihyperglycemic treatment in patients with type 2 diabetes in Italy: the impact of age and kidney function. Oncotarget. 2017; 8:62039–48.
https://doi.org/10.18632/oncotarget.18816
PMID:28977924

13. Kargulewicz A, Szulińska M, Kujawska-Łuczak M, Swora-Cwynar E, Musialik K, Grzymisławska M, Kręgielska-Narożna M, Bogdański P. Improvement of serum adiponectin and leptin concentrations: effects of a low-calorie or isocaloric diet combined with metformin or orlistat - a prospective randomized open-label trial. Eur Rev Med Pharmacol Sci. 2016; 20:3868–76. PMID:27735028

14. Umezawa S, Higurashi T, Nakajima A. AMPK: therapeutic target for diabetes and cancer prevention. Curr Pharm Des. 2017; 23:3629–44.
https://doi.org/10.2174/0929867324666170713150440 PMID:28714409

15. Tokubuchi I, Tajiri Y, Iwata S, Hara K, Wada N, Hashinaga T, Nakayama H, Mifune H, Yamada K. Beneficial effects of metformin on energy metabolism and visceral fat volume through a possible mechanism of fatty acid oxidation in human subjects and rats. PLoS One. 2017; 12:e0171293.
https://doi.org/10.1371/journal.pone.0171293
PMID:28158227

16. Chai TF, Hong SY, He H, Zheng L, Hagen T, Luo Y, Yu FX. A potential mechanism of metformin-mediated regulation of glucose homeostasis: inhibition of Thioredoxin-interacting protein (Txnip) gene expression. Cell Signal. 2012; 24:1700–05.
https://doi.org/10.1016/j.cellsig.2012.04.017
PMID:22561086

17. Yang X, Xu Z, Zhang C, Cai Z, Zhang J. Metformin, beyond an insulin sensitizer, targeting heart and pancreatic β cells. Biochim Biophys Acta Mol Basis Dis. 2017; 1863:1984–90.
https://doi.org/10.1016/j.bbadis.2016.09.019
PMID:27702625

18. Park SH, Lee J, Kang MA, Moon YJ, Wang SI, Kim KM, Park BH, Jang KY, Kim JR. Potential of l-thyroxine to differentiate osteoblast-like cells via Angiopoietin1. Biochem Biophys Res Commun. 2016; 478:1409–15.
https://doi.org/10.1016/j.bbrc.2016.08.137
PMID:27569283

19. Kostenuik PJ, Halloran BP, Morey-Holton ER, Bikle DD. Skeletal unloading inhibits the in vitro proliferation and differentiation of rat osteoprogenitor cells. Am J Physiol. 1997; 273:E1133–39.
https://doi.org/10.1152/ajpendo.1997.273.6.e1133
PMID:9435529

20. Wu Z, Ou L, Wang C, Yang L, Wang P, Liu H, Xiong Y, Sun K, Zhang R, Zhu X. Icaritin induces MC3T3-E1 subclone14 cell differentiation through estrogen receptor-mediated ERK1/2 and p38 signaling activation. Biomed Pharmacother. 2017; 94:1–9.
https://doi.org/10.1016/j.biopha.2017.07.07128742995

21. Qiao X, Nie Y, Ma Y, Chen Y, Cheng R, Yin W, Hu Y, Xu W, Xu L. Irisin promotes osteoblast proliferation and differentiation via activating the MAP kinase signaling pathways. Sci Rep. 2016; 6:18732.
https://doi.org/10.1038/srep18732 PMID:26738434

22. Ying Y, Ueta T, Jiang S, Lin H, Wang Y, Vavvas D, Wen R, Chen YG, Luo Z. Metformin inhibits ALK1-mediated angiogenesis via activation of AMPK. Oncotarget. 2017; 8:32794–806.
https://doi.org/10.18632/oncotarget.15825
PMID:28427181

23. Luo M, Tan X, Mu L, Luo Y, Li R, Deng X, Chen N, Ren M, Li Y, Wang L, Wu J, Wan Q. MiRNA-21 mediates the antiangiogenic activity of metformin through targeting PTEN and SMAD7 expression and PI3K/AKT pathway. Sci Rep. 2017; 7:43427.
https://doi.org/10.1038/srep43427 PMID:28230206

24. Kolb R, Phan L, Borcherding N, Liu Y, Yuan F, Janowski AM, Xie Q, Markan KR, Li W, Potthoff MJ, Fuentes-Mattei E, Ellies LG, Knudson CM, et al. Obesity-associated NLRC4 inflammasome activation drives breast cancer progression. Nat Commun. 2016; 7:13007.
https://doi.org/10.1038/ncomms13007
PMID:27708283

25. Arbeláez-Quintero I, Palacios M. To Use or Not to Use Metformin in Cerebral Ischemia: A Review of the Application of Metformin in Stroke Rodents. Stroke Res Treat. 2017; 2017:9756429.
https://doi.org/10.1155/2017/9756429
PMID:28634570

26. Jin Q, Cheng J, Liu Y, Wu J, Wang X, Wei S, Zhou X, Qin Z, Jia J, Zhen X. Improvement of functional recovery by chronic metformin treatment is associated with enhanced alternative activation of microglia/macrophages and increased angiogenesis and neurogenesis following experimental stroke. Brain Behav Immun. 2014; 40:131–42.
https://doi.org/10.1016/j.bbi.2014.03.003
PMID:24632338

27. Venna VR, Li J, Hammond MD, Mancini NS, McCullough LD. Chronic metformin treatment improves post-stroke angiogenesis and recovery after experimental stroke. Eur J Neurosci. 2014; 39:2129–38. https://doi.org/10.1111/ejn.12556 PMID:24649970

28. Li J, Benashski SE, Venna VR, McCullough LD. Effects of metformin in experimental stroke. Stroke. 2010; 41:2645–52. https://doi.org/10.1161/STROKEAHA.110.589697 PMID:20847317

29. Abdelsaid M, Prakash R, Li W, Coucha M, Hafez S, Johnson MH, Fagan SC, Ergul A. Metformin treatment in the period after stroke prevents nitrative stress and restores angiogenic signaling in the brain in diabetes. Diabetes. 2015; 64:1804–17. https://doi.org/10.2337/db14-1423 PMID:25524911

30. Janghorbani M, Van Dam RM, Willett WC, Hu FB. Systematic review of type 1 and type 2 diabetes mellitus and risk of fracture. Am J Epidemiol. 2007; 166:495–505. https://doi.org/10.1093/aje/kwm106 PMID:17575306

31. Moayeri A, Mohamadpour M, Mousavi SF, Shirzadpour E, Mohamadpour S, Amraei M. Fracture risk in patients with type 2 diabetes mellitus and possible risk factors: a systematic review and meta-analysis. Ther Clin Risk Manag. 2017; 13:455–68. https://doi.org/10.2147/TCRM.S131945 PMID:28442913

32. Montagnani A, Gonnelli S, Alessandri M, Nuti R. Osteoporosis and risk of fracture in patients with diabetes: an update. Aging Clin Exp Res. 2011; 23:84–90. https://doi.org/10.1007/BF03351073 PMID:21743287

33. Wolverton D, Blair MM. Fracture risk associated with common medications used in treating type 2 diabetes mellitus. Am J Health Syst Pharm. 2017; 74:1143–51. https://doi.org/10.2146/ajhp160319 PMID:28743778

34. Wang P, Ma T, Guo D, Hu K, Shu Y, Xu HH, Schneider A. Metformin Induces Osteoblastic Differentiation of Human Induced Pluripotent Stem Cell-derived Mesenchymal Stem Cells. J Tissue Eng Regen Med. 2018; 12:437–46. https://doi.org/10.1002/term.2470 PMID:28494141

35. Shao X, Cao X, Song G, Zhao Y, Shi B. Metformin rescues the MG63 osteoblasts against the effect of high glucose on proliferation. J Diabetes Res. 2014; 2014:453940. https://doi.org/10.1155/2014/453940 PMID:24812633

36. Jaiswal RK, Jaiswal N, Bruder SP, Mbalaviele G, Marshak DR, Pittenger MF. Adult human mesenchymal stem cell differentiation to the osteogenic or adipogenic lineage is regulated by mitogen-activated protein kinase. J Biol Chem. 2000; 275:9645–52. https://doi.org/10.1074/jbc.275.13.9645 PMID:10734116

37. Suzuki A, Palmer G, Bonjour JP, Caverzasio J. Regulation of alkaline phosphatase activity by p38 MAP kinase in response to activation of Gi protein-coupled receptors by epinephrine in osteoblast-like cells. Endocrinology. 1999; 140:3177–82. https://doi.org/10.1210/endo.140.7.6857 PMID:10385412

38. Suzuki A, Guicheux J, Palmer G, Miura Y, Oiso Y, Bonjour JP, Caverzasio J. Evidence for a role of p38 MAP kinase in expression of alkaline phosphatase during osteoblastic cell differentiation. Bone. 2002; 30:91–98. https://doi.org/10.1016/S8756-3282(01)00660-3 PMID:11792570

39. Greenblatt MB, Shim JH, Zou W, Sitara D, Schweitzer M, Hu D, Lotinun S, Sano Y, Baron R, Park JM, Arthur S, Xie M, Schneider MD, et al. The p38 MAPK pathway is essential for skeletogenesis and bone homeostasis in mice. J Clin Invest. 2010; 120:2457–73. https://doi.org/10.1172/JCI42285 PMID:20551513

40. Rodríguez-Carballo E, Gámez B, Sedó-Cabezón L, Sánchez-Feutrie M, Zorzano A, Manzanares-Céspedes C, Rosa JL, Ventura F. The p38α MAPK function in osteoprecursors is required for bone formation and bone homeostasis in adult mice. PLoS One. 2014; 9:e102032. https://doi.org/10.1371/journal.pone.0102032 PMID:25007355

41. Ge C, Yang Q, Zhao G, Yu H, Kirkwood KL, Franceschi RT. Interactions between extracellular signal-regulated kinase 1/2 and p38 MAP kinase pathways in the control of RUNX2 phosphorylation and transcriptional activity. J Bone Miner Res. 2012; 27:538–51. https://doi.org/10.1002/jbmr.561 PMID:22072425

42. Ortuño MJ, Ruiz-Gaspà S, Rodríguez-Carballo E, Susperregui AR, Bartrons R, Rosa JL, Ventura F. p38 regulates expression of osteoblast-specific genes by phosphorylation of osterix. J Biol Chem. 2010; 285:31985–94. https://doi.org/10.1074/jbc.M110.123612 PMID:20682789

43. Ortuño MJ, Susperregui AR, Artigas N, Rosa JL, Ventura F. Osterix induces Col1a1 gene expression through binding to Sp1 sites in the bone enhancer and proximal promoter regions. Bone. 2013; 52:548–56. https://doi.org/10.1016/j.bone.2012.11.007 PMID:23159876

44. Artigas N, Ureña C, Rodríguez-Carballo E, Rosa JL, Ventura F. Mitogen-activated protein kinase (MAPK)-

regulated interactions between Osterix and Runx2 are critical for the transcriptional osteogenic program. J Biol Chem. 2014; 289:27105–17. https://doi.org/10.1074/jbc.M114.576793 PMID:25122769

45. Manolagas SC. Role of cytokines in bone resorption. Bone. 1995 (Suppl); 17:63S–67S. https://doi.org/10.1016/8756-3282(95)00180-L PMID:8579900

46. Kotake S, Sato K, Kim KJ, Takahashi N, Udagawa N, Nakamura I, Yamaguchi A, Kishimoto T, Suda T, Kashiwazaki S. Interleukin-6 and soluble interleukin-6 receptors in the synovial fluids from rheumatoid arthritis patients are responsible for osteoclast-like cell formation. J Bone Miner Res. 1996; 11:88–95. https://doi.org/10.1002/jbmr.5650110113 PMID:8770701

47. Tamura T, Udagawa N, Takahashi N, Miyaura C, Tanaka S, Yamada Y, Koishihara Y, Ohsugi Y, Kumaki K, Taga T. Soluble interleukin-6 receptor triggers osteoclast formation by interleukin 6. Proc Natl Acad Sci USA. 1993; 90:11924–28. https://doi.org/10.1073/pnas.90.24.11924 PMID:8265649

48. Mori T, Miyamoto T, Yoshida H, Asakawa M, Kawasumi M, Kobayashi T, Morioka H, Chiba K, Toyama Y, Yoshimura A. IL-1β and TNFα-initiated IL-6-STAT3 pathway is critical in mediating inflammatory cytokines and RANKL expression in inflammatory arthritis. Int Immunol. 2011; 23:701–12. https://doi.org/10.1093/intimm/dxr077 PMID:21937456

49. Son HJ, Lee J, Lee SY, Kim EK, Park MJ, Kim KW, Park SH, Cho ML. Metformin attenuates experimental autoimmune arthritis through reciprocal regulation of Th17/Treg balance and osteoclastogenesis. Mediators Inflamm. 2014; 2014:973986. https://doi.org/10.1155/2014/973986 PMID:25214721

50. Molinuevo MS, Schurman L, McCarthy AD, Cortizo AM, Tolosa MJ, Gangoiti MV, Arnol V, Sedlinsky C. Effect of metformin on bone marrow progenitor cell differentiation: in vivo and in vitro studies. J Bone Miner Res. 2010; 25:211–21. https://doi.org/10.1359/jbmr.090732 PMID:19594306

51. Shah M, Kola B, Bataveljic A, Arnett TR, Viollet B, Saxon L, Korbonits M, Chenu C. AMP-activated protein kinase (AMPK) activation regulates in vitro bone formation and bone mass. Bone. 2010; 47:309–19. https://doi.org/10.1016/j.bone.2010.04.596 PMID:20399918

52. Mai QG, Zhang ZM, Xu S, Lu M, Zhou RP, Zhao L, Jia CH, Wen ZH, Jin DD, Bai XC. Metformin stimulates osteoprotegerin and reduces RANKL expression in osteoblasts and ovariectomized rats. J Cell Biochem. 2011; 112:2902–09. https://doi.org/10.1002/jcb.23206 PMID:21618594

53. Gao Y, Li Y, Xue J, Jia Y, Hu J. Effect of the anti-diabetic drug metformin on bone mass in ovariectomized rats. Eur J Pharmacol. 2010; 635:231–36. https://doi.org/10.1016/j.ejphar.2010.02.051 PMID:20307532

54. Araújo AA, Pereira AS, Medeiros CA, Brito GA, Leitão RF, Araújo LS, Guedes PM, Hiyari S, Pirih FQ, Araújo Júnior RF. Effects of metformin on inflammation, oxidative stress, and bone loss in a rat model of periodontitis. PLoS One. 2017; 12:e0183506. https://doi.org/10.1371/journal.pone.0183506 PMID:28847008

55. Jeyabalan J, Viollet B, Smitham P, Ellis SA, Zaman G, Bardin C, Goodship A, Roux JP, Pierre M, Chenu C. The anti-diabetic drug metformin does not affect bone mass in vivo or fracture healing. Osteoporos Int. 2013; 24:2659–70. https://doi.org/10.1007/s00198-013-2371-0 PMID:23644877

56. Bak EJ, Park HG, Kim M, Kim SW, Kim S, Choi SH, Cha JH, Yoo YJ. The effect of metformin on alveolar bone in ligature-induced periodontitis in rats: a pilot study. J Periodontol. 2010; 81:412–19. https://doi.org/10.1902/jop.2009.090414 PMID:20192868